Journal of Controlled Release 270 (2018) 135–144

Contents lists available at ScienceDirect

Journal of Controlled Release

journal homepage: www.elsevier.com/locate/jconrel

Nanoparticulate peptide delivery exclusively to the brain produces tolerance free analgesia

Lisa Godfrey[a], Antonio Iannitelli[a], Natalie L. Garrett[c], Julian Moger[c], Ian Imbert[d], Tamara King[d], Frank Porreca[e], Ramesh Soundararajan[a], Aikaterini Lalatsa[a,f], Andreas G. Schätzlein[a,b], Ijeoma F. Uchegbu[a,b,*]

[a] UCL School of Pharmacy, 29-39 Brunswick Square, London WC1N 1AX, UK
[b] Nanomerics Ltd., 1394 High Road, London N20 9YZ, UK
[c] School of Physics, University of Exeter, Stocker Road, Exeter EX4 4QL, UK
[d] Department of Biomedical Sciences, College of Osteopathic Medicine, University of New England, 11 Hills Beach Rd, Biddeford, ME 04005, USA
[e] Department of Pharmacology, College of Medicine, University of Arizona, 1501 N. Campbell Ave, Tucson, AZ 85724, USA
[f] Department of Pharmaceutics, School of Pharmacy and Biomedical Sciences, University of Portsmouth, St Michael's Building 5.05, White Swan Road, Portsmouth PO1 2DT, UK

ARTICLE INFO

Keywords:
Nanoparticles
Microparticles
Chitosan amphiphiles
Leucine[5]-enkephalin
Intranasal
Analgesia
Brain delivery
Delta opioid receptor

ABSTRACT

The delivery of peptide drugs to the brain is challenging, principally due to the blood brain barrier and the low metabolic stability of peptides. Exclusive delivery to the brain with no peripheral exposure has hitherto not been demonstrated with brain quantification data. Here we show that polymer nanoparticles encapsulating leucine[5]-enkephalin hydrochloride (LENK) are able to transport LENK exclusively to the brain via the intranasal route, with no peripheral exposure and nanoparticle localisation is observed within the brain parenchyma. Animals dosed with LENK nanoparticles (NM0127) showed a strong anti-nociceptive response in multiple assays of evoked and on going pain whereas animals dosed intranasally with LENK alone were unresponsive. Animals did not develop tolerance to the anti-hyperalgesic activity of NM0127 and NM0127 was active in morphine tolerant animals. A microparticulate formulation of clustered nanoparticles was prepared to satisfy regulatory requirements for nasal dosage forms and the polymer nanoparticles alone were found to be biocompatible, via the nasal route, on chronic dosing.

1. Introduction

The delivery of peptides to the brain is challenging, not merely because of the blood brain barrier but also because peptides have a very short plasma half life and are frequently not detected in the plasma on intravenous administration [1]. The intranasal to brain route of administration has emerged as an interesting route for the administration of compounds directly into the brain [2] even though the dose (100 μL or 25 mg) is a limitation. Here we show that the use of an intranasal nanoparticle delivery system enables the delivery of a metabolically unstable [3], δ selective opioid receptor (DOR) [4][5] agonist, leucine[5]-enkephalin hydrochloride (LENK), directly and exclusively to the brain. The δ selectivity has been well studied by Toll and others [5] using cloned human μ, δ and κ receptors in Chinese Hamster Ovary (CHO) cells with EC50 values, in ^{35}SGTPγS binding assays, of 25.5 ± 0.8 nM and 1.35 ± 0.2 nM for μ-CHO and δ-CHO cell membranes respectively. Similar results were obtained with guinea pig brain membranes with Ki values of 21.7 ± 1.4 nm and 1.6 ± 0.5 nm obtained when using the μ (^{3}H DAMGO) and δ (^{3}H DPDPE) selective agonists respectively [5]. DORs reside in the cerebral cortex, putamen, caudate nucleus, nucleus accumbens and hippocampus of humans [6] and hence exclusive brain delivery, via a non-parenteral route of administration, enables LENK to be considered as a potential analgesic. Chronic pain affects 19% of European adults, with nearly half being poorly managed by current therapies and with devastating consequences on their quality of life [7]. While neuropathic pain (diabetic, post herpetic or human immunodeficiency virus related) affects 6 million patients in the seven major markets (United States, Japan, France, Germany, Italy, Spain and the UK), only 25% of these patients experience pain relief with the current approved medicines [8]. Furthermore breakthrough pain is highly prevalent in analgesic treated cancer patients with one study reporting prevalence rates of 74% [9] and 45% of the patients studied were unable to predict the onset of excruciating breakthrough pain [9]. Breakthrough pain requires remedies with a rapid onset of action.

* Corresponding author at: UCL School of Pharmacy, 29-39 Brunswick Square, London WC1N 1AX, UK.
E-mail address: Ijeoma.uchegbu@ucl.ac.uk (I.F. Uchegbu).

https://doi.org/10.1016/j.jconrel.2017.11.041
Received 18 October 2017; Received in revised form 24 November 2017; Accepted 25 November 2017
Available online 27 November 2017

Opiates acting predominantly at mu opioid receptors (MORs) have been used to treat both chronic and acute pain for thousands of years [10] although the side effects of these medicines (constipation, nausea, drowsiness, dependence and respiratory depression) [11] often limit their use. The endogenous opioids, i.e. the enkephalins, have been studied but not developed as drugs, due to their rapid enzymatic degradation and poor brain permeation [12–14], despite the use of various penetration enhancers [15,16]. However enkephalinase inhibitors have been trialled in the clinic [17].

The nose to brain route has been advocated as a delivery route for labile and high molecular weight drugs to the brain in humans [2,18], as drugs can access the brain directly through the olfactory neurons as well as avoid first pass liver metabolism and gastrointestinal degradation. However such intranasal dosage forms must also avoid the degradative enzymes (e.g. carboxypeptidases and cytochrome P450) present in the human nasal cavity [19,20]. Administration of drugs to the nasal cavity is also a means of achieving systemic exposure due to the highly vascularised respiratory epithelium, which enables absorption of drugs into the blood through paracellular or transcellular epithelial and endothelial pathways and there are products on the market that are delivered nasally to achieve systemic exposure, including peptides [21]. While delivery to only the brain via the intranasal route, has been inferred by others [2], here we demonstrate exclusive delivery of a low molecular weight and metabolically labile peptide, leucine^5-enkephalin (Molecular weight = 556 Da), to the brain on intranasal administration and when formulated as a nanoparticle with no peripheral exposure or activity. The peptide is of pharmaceutical interest as a possible pain therapeutic.

2. Materials and methods

2.1. Materials

All reagents and chemicals were obtained from Sigma Aldrich Chemical Co, UK, unless otherwise stated. All solvents and acids were obtained from Fisher Scientific, Loughborough, UK. Dialysis membranes were purchased from Medicell International Ltd., UK. Deuterium oxide, Methanol-d_6 and deuterated palmitic acid (palmitic acid-d_{31}) were obtained from Cambridge Isotope Laboratories Inc. UK. Leucine^5-Enkephalin hydrochloride was obtained from CELTEK Bioscience, USA. Morphine sulphate and Isoflurane were purchased from Centaur Services Ltd., UK. Water for injection and saline were obtained from AAH pharmaceuticals Ltd., Coventry, UK. Naloxone hydrochloride MP Biomedicals, USA. Nanomerics' Molecular Envelope Technology (GCPQ – *N*-palmitoyl-*N*-monomethyl-*N*,*N*-dimethyl-*N*,*N*,*N*-trimethyl-6-O-glycolchitosan) was obtained from Nanomerics Ltd. All reagents and chemicals were used without further purification and were ≥ 99% purity. Animals were purchased from Harlan, UK or Harlan, USA (CPP animals only) and PE10 tubing was purchased from Smiths Medical, UK.

2.2. Methods

2.2.1. NM0127 nanoparticles

NM0127 nanoparticles were prepared from GCPQ (*N*-palmitoyl-*N*-monomethyl-*N*,*N*-dimethyl-*N*,*N*,*N*-trimethyl-6-O-glycolchitosan, Mw = 18.6 ± 4.6 kDa, Mw/Mn = 1.033 ± 0.027, mole% palmitoylation = 15 ± 1.3, mole% quaternary ammonium groups = 8 ± 0.8) and LENK by vortexing for 5 min in water for injection BP, the pH adjusted to pH = 5.8 with NaOH (1 M) prior to probe sonicating (Qsonica, UK) with the instrument set at 30% of its maximum output for 10 min on ice. For the CFA and CPP studies the GCPQ had the following characteristics: Mw = 18.0 ± 3.7 kDa, Mw/Mn = 1.029 ± 0.023, mole% palmitoylation = 16 ± 3.6, mole% quaternary ammonium groups = 10 ± 2.2. NM0127 formulations for intranasal, intravenous and oral use had a GCPQ, LENK weight ratio of 1, 2.3 and 5 respectively. Particle sizing was carried out with a Malvern Zetasizer 3000HS (Malvern Instruments, UK) at 25 °C and a wavelength of 633 nm with data analysed using the Contin method.

NM0127 was imaged by transmission electron microscopy (TEM). A drop of NM0127 was placed on Formvar/Carbon Coated Grid (F1961100 3.05 mm, Mesh 300, Tab Labs Ltd., UK), stained (aqueous Uranyl Acetate - 1% w/v) and imaged (FE1 CM120 BioTwin Microscope equipped with an AMT digital camera, Thermofisher Scientific, UK).

2.2.2. Peptide analysis

LENK analysis was performed on an Agilent high performance liquid chromatography (HPLC) system (Agilent Technologies, UK) consisting of a binary pump (1220 Infinity LC Gradient System VL) equipped with a variable wavelength UV detector (λ = 214 nm) and an Onyx monolithic C18 column (5 μm particle size, 4.6 mm × 10 mm) with a C18 guard column (Phenomenex, UK). Mobile phase = water, acetonitrile, trifluoroacetic acid (81.98: 18: 0.02), flow rate = 1 mL min^{-1}, column temperature = 30 °C, injection volume = 10 μL, LENK retention time = 6.6 min, calibration curve for quantification (y = 14.6 ± 1.1, r^2 = 0.999 ± 0.002, n = 11 separate experiments), lower limit of quantification = 5 μg mL^{-1}. Data analysis was via Agilent Chemstation. NM0127 formulations were diluted in mobile phase, filtered (0.22 μm) and the filtrate analysed by HPLC.

2.2.3. NM0127 Nano-in-micro formulations

NM0127 Nano-in-Micro formulations were prepared from LENK and GCPQ (Mw = 11.2 kDa, Mw/Mn = 1.01, Mole% palmitoylation = 23, Mole% quaternary ammonium groups = 12) in distilled water (20 mL) at a total solid concentration of 10% w/v and a GCPQ, LENK ratio of 1 g g^{-1}. The suspension was subjected to high pressure homogenisation (EmulsiFlex C5, Avestin, Germany, 1 cycle at 18000 Psi) and the resulting nanoparticles spray dried to give NM0127 nano-in-micro particles (Büchi Nano Spray Dryer B290 equipped with ultrasonics, Büchi Labortechnik AG, Switzerland, inlet temperature = 180 °C, outlet temperature = 120 °C, nozzle temperature = 60 °C, aspirator flow rate = 36 m^3 h^{-1}, spray rate = 1 mL min^{-1}, power at the nozzle = 1.8 watts). Particle sizing was via an Helos sizer (Sympatec GmbH, Germany), peptide analysis by HPLC and particle imaging achieved using an FEI Quanta 200 F scanning electron microscope (ThermoFisher Scientific, The Netherlands).

X-ray diffraction analyses were carried out using a Rigaku MiniFlex 600 diffractometer (Rigaku, UK) with a voltage of 40 kV, a current of 15 mA. Patterns were obtained using a step width of 0.02 deg. with a detector resolution in 2θ (diffraction angle) between 2 deg. and 60 deg.

NM0127 microparticles (4 mg) were dispersed in water (0.1 mL) and gently shaken for 10 min to regenerate the nanoparticles and the nanoparticles imaged by TEM.

2.2.4. Animals

Male Sprague Dawley rats (weight = 200–275 g for the behavioural studies and 130–170 g for the pharmacokinetics studies) were housed four per cage in an air conditioned unit (20–22 °C, 50–60% humidity) and allowed free access to standard rodent chow and water. Lighting was controlled on a twelve-hour cycle (on at 07.00 h and out at 19.00 h). Animals were habituated for 7 days prior to experimentation and acclimatised to the procedure room for 1 h prior to testing. All protocols were conducted under a UK Home Office licence and approved by a local ethics committee with the exception of CPP studies which were reviewed and approved by the Institutional Animal Care and Use Committee of the University of New England, and were carried out in compliance National Institutes of Health guidelines. Animals were randomised prior to all experiments using the Latin Square method (behavioural studies) or by weight (pharmacokinetics and imaging studies) and all behavioural experiments assessed by an operator blinded to the treatment by assigning the animals codes and the dosing then carried out in order of the codes. The data analysis also done with code identifiers or by a separate operator. This was except for

the CPP studies, which were video monitored. Sample sizes were chosen based on either power calculations after a pilot study to determine the standard deviation (all behavioural experiments) or after a pilot study (pharmacokinetics experiments).

2.2.5. Anti-nociception hot plate test

Prior to dosing rats were placed on a hot plate to ascertain the baseline levels of residency prior to an escape attempt (a jump or a lick of the paw) and for a maximum time of 30 s. Rats were dosed with various intravenous and oral doses of NM0127 and control animals dosed the relevant vehicle.

At various intervals after dosing, rats were then placed on the hot plate for a maximum of 30 s and the time to escape attempt recorded. Anti-nociception was recorded as the difference between the hotplate residency time before and after dosing.

2.2.6. Intranasal dosing and dose response analysis

For the Complete Freund's Adjuvant and conditioned placement preference studies, rats were intranasally administered with water for injection, intranasal LENK or various doses of NM0127. Animals were briefly anesthetised with isoflurane and intranasally administered the formulation using an insulin syringe attached to PE10 tubing (15 mm), the tubing was inserted into one of nares [22].

2.2.7. Complete Freund's adjuvant induced tactile hypersensitivity

Rats received an intraplantar injection of Complete Freund's adjuvant (CFA). CFA induced hind paw oedema and tactile hypersensitivity were evaluated 24 h after the CFA injection [23]. Rats were individually placed on an elevated plastic mesh (0.5 cm^2 perforations) in a clear plastic cage. Two habituations to the evaluation chambers for at least 5 min duration each were performed on two different days. A baseline measurement was taken on test day pre-CFA. Tactile hypersensitivity was assessed by the sensitivity to the application of von Frey filaments (Ugo Basile, Italy). The von Frey filaments (1.4, 2, 4, 6, 8, 10, 15, 26 g) were presented perpendicularly to the plantar surface of the injected paw in ascending order, and held in this position for 5 s with enough force to cause a slight bend in the filament. Positive responses, included an abrupt withdrawal of the hind paw or a flinching on application of the hair. Once a positive withdrawal response was established, the paw was retested, starting with the next descending von Frey hair until no response occurred. The lowest amount of force required to elicit a response was recorded as the paw withdrawal force (g) [24].

Tactile hypersensitivity was defined as a significant decrease in withdrawal thresholds to von Frey filament application.

To test the formulation effects on tactile hypersensitivity, rats were evaluated for thresholds 24 h after CFA injection; they were then randomised according to their threshold values and administered with formulations. Once the evaluation was complete, rats were returned to their home cage for 3 days and then thresholds were reassessed on day 5 post the CFA injection.

2.2.8. Central and peripheral contributions to anti-hyperalgesia

24 h after a CFA injection, non-selective opioid antagonists (naloxone hydrochloride and naloxone methiodide) were administered subcutaneously (to enable unfettered access of naloxone and naloxone methiodide to the central and peripheral opioid receptors) and concomitantly with intranasal NM0127 in water and paw withdrawal thresholds assessed.

2.2.9. Analgesic tolerance and analgesic cross tolerance to morphine

Intranasal NM0127 in water was administered and the paw withdrawal threshold assessed. Subsequently the same dose of NM0127 was administered intranasally to the same animals twice a day (9 am, 2 pm) for 4 days. The paw withdrawal thresholds were reassessed after the administration of a final dose on day 5. Morphine sulphate was administered subcutaneously as a positive control.

To assess the development of cross tolerance to morphine, subcutaneous morphine sulphate was administered to two groups of animals and the paw withdrawal thresholds were assessed. Subsequently both groups of animals were administered morphine sulphate twice a day (9 am and 2 pm) for 4 days and on Day 5, intranasal NM0127 in water was administered to one group of morphine dosed animals, while subcutaneous morphine sulphate was administered to the second group of morphine dosed animals, and the paw withdrawal threshold re-assessed for both groups. Subcutaneous and intranasal PBS were administered to control animals on Days 1 and 5 respectively.

2.2.10. Spinal nerve ligation (SNL) and conditioned placement preference (CPP) studies

Spinal nerve ligation (SNL) at L5 and L6 was induced using the procedure of Kim and Chung [25]. Sprague Dawley rats were anesthetized with 2% isoflurane. A 3 cm longitudinal incision, 5 mm lateral from the midline was made at the lower lumber and sacral levels. The location of the incision is determined by the position of the L5 spinous process. Connective tissues, remaining muscle and L6 spinous processes were removed, the L5 and L6 spinal nerves freed from the adjacent structure, and the nerves tightly ligated with 4–0 silk suture. Haemostasis was confirmed, the muscles sutured in layers and the wound closed. Sham control rats underwent the same operation and handling as the experimental animals but without actual ligation. 7 days post-surgery the absence and presence of hypersensitivity was confirmed in Sham and SNL animals respectively by von Frey filaments as described above.

Conditioned place preference (CPP) was performed using a modification of the single trial conditioning procedure previously described [26,27]. On day 13 post surgery rats underwent a 1 day habituation in which they were placed in the CPP boxes and allowed to explore all chambers. Behaviour was recorded and analysed to verify that no chamber bias existed to the conditioning chambers, as defined by spending < 180 s or > 720 s in one of the chambers. Animals exhibiting a chamber bias ($< 3\%$ of total animals tested for CPP, i.e. 1 animal) were removed from the study. The following day (conditioning day), all rats (Sham and SNL) received an intranasal dose of the vehicle, under short term isoflurane anaesthesia and were immediately (within 2 min) confined to the appropriate pairing chamber for 30 min in the morning. Animals were removed and placed in their home cages for 4 h. For the afternoon session animals received intranasal NM0127 in water under short term isoflurane anaesthesia and were immediately (within 2 min) confined to the opposite chamber for 30 min. On the test day, 20 h following the afternoon pairing, rats were placed in the CPP box with access to all chambers and their behaviour video recorded for 15 min. Significantly increased post-conditioning time spent in the drug-paired chamber, as compared to pre-conditioning time, indicates a CPP. Decreased post-conditioning time spent in the drug paired chamber, as compared to the pre-conditioning time, indicates conditioned place aversion. No change between the time spent in the drug-paired chamber, as compared to pre-conditioning time, indicates no conditioned place preference or aversion.

2.2.11. Pharmacokinetics

Male Sprague Dawley rats weighing 145–180 g ($n = 6$) were briefly anesthetised with isoflurane and intranasally administered either no treatment, LENK or NM0127 in water.

At various time points, animals were killed with an intraperitoneal overdose of pentobarbital and the brains removed, separated from the olfactory bulb and cerebellum and the cerebrum washed in phosphate buffered saline (PBS, pH = 7.4). Cerebrum and olfactory bulb tissues were immediately snap frozen in liquid Nitrogen and analysed on the same day of sampling. After the pentobarbital overdose, blood samples were also taken by cardiac puncture and collected into EDTA vacutainer tubes. Protease inhibitor cocktail (10 μL, Sigma, UK) was added to each

tube and the tubes inverted. Plasma was separated by centrifugation (2000*g* × 15 min, 4 °C) and plasma samples were stored at − 80 °C until analyses could be performed on them.

An aliquot of the plasma sample (500 μL) was mixed with an equal volume of the extraction medium (1 M acetic acid, 0.02 M HCL, 1% mercaptoethanol) and to this was added the internal standard (dalargin, 10 μg mL^{-1}, 10 μL) and protease inhibitor cocktail (10 μL). The plasma samples were centrifuged (6800*g* for 30 min at 4 °C) and to the supernatant was added trichloroacetic acid (TCA, 50%w/v, 200 μL) and the resulting mixture centrifuged again (6800*g* for 30 min at 4 °C). The supernatant was then extracted with diethyl ether (3 × 1 mL each time) and the aqueous layer freeze dried. The freeze dried residue was reconstituted in formic acid (0.1% w/v, 200 μL), filtered (0.2 μm) and the filtrate analysed by LC-MS.

Plasma calibration curve standards were prepared, by extracting spiked plasma (500 μL), which had been diluted with an equal volume of extraction medium (LENK = 1–100 ng mL^{-1}, dalargin = 100 ng mL^{-1}, $y = 51.19x + 720.89$, $r^2 = 0.97$).

To every 1.3 g of fresh cerebrum sample was added 13 mL of TCA (50% w/v) followed by the addition of protease inhibitor cocktail (1 mL). Brain samples were then homogenised and aliquots (1 mL) of this homogenate spiked with dalargin (10 μg mL^{-1}, 10 μL), centrifuged (10,000*g* × 30 min, 4 °C) and to an aliquot of the supernatant (800 μL) was added TCA (50% w/v, 160 μL). The mixture was centrifuged again (10,000*g* for 30 min at 4 °C) and the supernatant extracted with diethyl ether (3 × 1 volume). An aliquot of the resulting aqueous phase (500 μL) was freeze-dried. The freeze-dried sample was reconstituted in formic acid (0.1% v/v, 200 μL) and analysed by LC-MS.

For the brain calibration curve, to each 1.3 g of tissue was added to 13 mL of TCA (50% v/v), followed by protease inhibitor cocktail (1 mL); the brain samples homogenised and aliquots (1 mL) used to construct a standard curve after extraction as detailed above (LENK = 1–1000 ng mL^{-1}, dalargin = 100 ng mL^{-1}, $y = 0.0046x + 0.232$, $r^2 = 0.998$).

Fresh olfactory bulb samples were weighed and TCA (50% v/v, 2 mL) added followed by the protease inhibitor cocktail (100 μL). The samples were then homogenised and to aliquots of this homogenate (1 mL) were added dalargin (10 μg mL^{-1}, 10 μL), the sample centrifuged (10,000*g* × 30 min, 4 °C) and to the supernatant (800 μL) added TCA (50% v/v, 160 μL). The supernatant was then again centrifuged (10,000*g* × 30 min, 4 °C) and the resulting supernatant extracted with diethyl ether (3 × 1 volume). An aliquot of the resulting aqueous phase (500 μL) was freeze-dried. The freeze-dried sample was reconstituted in formic acid (0.1%, 200 μL) and analysed by LC - MS.

Olfactory bulb calibration standards were prepared by adding 6 mL of TCA (50% v/v) to 150 mg of tissue, followed by the addition protease inhibitor cocktail (100 μL). The samples were then homogenised and aliquots (1 mL) used to construct a standard curve after extraction as detailed above (LENK = 1–600 ng g^{-1}, dalargin = 100 ng mL^{-1}, $y = 0.0265x + 0.176$, $r^2 = 0.995$).

LC-MS/MS analysis was carried out using an Agilent 1260 infinity LC system (Agilent Technologies, Berkshire, UK) interfaced directly with Agilent 6460 triple quadrupole. Samples were separated on a reverse phase C18 Zorbax column (2.1 × 50 mm, 5 μm particle size) in a gradient mode with formic acid (FA, 0.1% w/v), acetonitrile: t_0 = 95% FA, t_5 = 70% FA, $t_{5.5}$ = 5% FA, $t_{6.5}$ = 5% FA, t_7 = 95% FA. Mobile phase flow rate = 0.3 mL min^{-1}, column temperature = 30 °C, injection volume = 10 μL, run time = 10 min. The retention times for dalargin and LENK were 4.6 min, 5.6 min respectively. The samples were ionized by electrospray ionization (ESI) in a positive ion mode. The electrospray parameters were as follows: electrospray capillary voltage = 3.5 kV, source temperature = 300 °C, ESI source = nitrogen, gas flow = 5 L min^{-1}, ion detection = Multiple Reaction Monitoring mode (Table 1).

2.2.12. Multiphoton microscopy

Deuterated GCPQ (dGCPQ) was supplied by Nanomerics Ltd. and dGCPQ nanoparticles synthesised as previously described [15]. Rats were intranasally dosed with dGCPQ and were subsequently killed at various time points, brains harvested and stored in neutral buffered formalin [(formaldehyde - 4% v/v, sodium phosphate monobasic – 0.4% w/v, sodium phosphate dibasic – 0.65% w/v) 60 mL]. All samples for multiphoton imaging were prepared as described previously and imaging carried out as described previously [15,28]. Nuclear membranes were identified as they were less lipid rich than the cell cytoplasm and appear darker in the image. Myelin sheaths around the neurons are lipid rich and appear brighter in the image and the cell membrane is lipid rich and appears brighter in the image.

2.2.13. Intranasal GCPQ good laboratory practice toxicology studies

Groups of male (n = 10) and female (n = 10) Sprague Dawley rats (starting weight 200–230 g for females and 320–340 g for males) were intranasally dosed (0.2 mL kg^{-1}/day dosed in 4 separate doses/day) with GCPQ nanoparticles in water for injection daily for 28 days and at three dose levels: a) 12 mg kg^{-1}, b) 18 mg kg^{-1} and c) 24 mg kg^{-1}. Groups of male (n = 10) and female (n = 10) Sprague Dawley rats were administered water for injection at the same dose volume as the test animals. The doses were given using a micropipette with attached appropriately sized plastic tip. All animals received 4 instillations into each nostril of either the control or the test item for a total of 0.2 mL on each treatment day. During dosing, the rats were held with their head in a vertical position. The micropipette was kept approximately 0.5 mm into the first nostril and the 0.025 mL drop of formulation was instilled. Immediately afterwards the second nostril was instilled. The animal was kept vertical for a few seconds to allow the formulation to disappear into the nose and then put back in its cage. Animals were weighed daily, food consumption monitored and examined for general condition prior to and after each dose with the eyes monitored periodically after the application of a mydriatic agent (1% Tropicamide). Blood was collected from the orbital sinus under isoflurane anaesthesia using a capillary tube and blood chemistry and haematology parameters determined. Urine was collected over an 18 h period, where the animals had no access to food but access to water and urine analysis carried out. At the end of the study, animals were killed using carbon dioxide, were subject to a full necropsy examination and histology samples examined.

2.2.14. Statistical analysis

Data were analysed by one or two-way analysis of variance (ANOVA) followed by Bonferroni post hoc test (equal variance) and Greenhouse-Geisser correction with Games Howell post hoc test if there was unequal variance. All statistical analyses were performed using SPSS (IBM, UK) and Graphpad Prism (GraphPad Inc., USA). *P* values < 0.05 were considered significant. For the conditioned placement preference experiments, data were analysed using a 2-factor analysis of variance (ANOVA: pre vs post conditioning by treatment group). Post hoc analysis was performed using Bonferroni tests.

2.2.15. Data and materials

Data and materials are available to readers by writing to the corresponding author.

3. Results and discussion

There is undoubtedly an unmet clinical need for efficacious analgesics. The current opioids are efficacious in the treatment of severe pain but are limited by the prevalence and severity of their side effects [11]. An endogenous peptide with analgesic properties and minimal side effects could certainly provide benefit to patients suffering from severe pain. However the delivery of peptides to the brain is not entirely without its own challenges. Our work demonstrates that we have

Table 1
LC-MS/MS analytical conditions.

Name	Precursor ion	Product ion	Dwell time	Frag (V)	CE (V)	Cell Acc (V)	Polarity
Dalargin	726	120	200	175	70	4	Positive
LENK	556	278.1	200	150	20	4	Positive

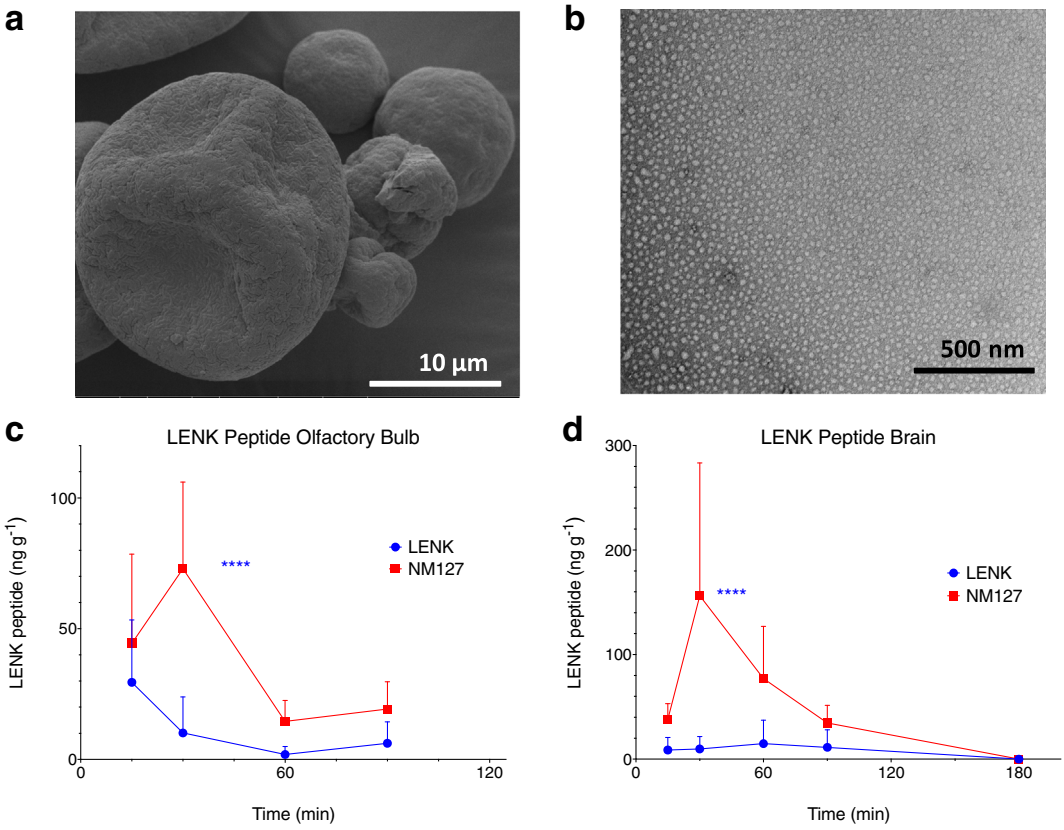

Fig. 1. NM0127 formulation morphology (a and b) and kinetics after nose-to-brain administration in male Sprague Dawley (SD) rats (c and d).
a) Scanning electron microscopy image of freshly prepared NM0127 microparticles (GCPQ, LENK ratio = 1: 1 g g^{-1}).
b) Transmission electron microscopy image of NM0127 nanoparticles reconstituted from microparticles (a) in water (LENK concentration = 30 mg mL^{-1}).
c and d) Concentration of LENK (mean ± s.d. n = 6) in the olfactory bulb (c) and cerebrum (d) following the administration of LENK (23 mg Kg^{-1}, 50 mg mL^{-1}) in NM0127 nanoparticles (LENK, GCPQ ratio = 1 g g^{-1}) or as the peptide alone. LENK was not detected in the plasma (n = 6 per time point) at any of the time points studied (15, 30, 60 and 120 min). **** = statistically significant differences between both groups ($p < 0.0001$). Images in Fig. 1a and b are representative images from 3 experiments. Data in Fig. 1c and d are representative data from 3 replicated experiments.

solved this peptide delivery problem. We tested the hypothesis that the encapsulation of an endogenous peptide with analgesic activity [29], within nanoparticles (that may be further formulated as microparticles), would lead to peptide brain delivery and analgesia.

LENK is formulated with *N*-palmitoyl-*N*-monomethyl-*N*,*N*-dimethyl-*N*,*N*,*N*-trimethyl-6-O-glycolchitosan (GCPQ) into a mixture of single 30 nm–40 nm nanoparticles and aggregated 100–200 nm nanoparticles (NM0127). The nanoparticles, in turn, are formulated into microparticles (volume mean diameter = 22.2 ± 0.96 µm, D_{10} = 11.07 ± 0.82 µm, D_{50} = 20.12 ± 1.14 µm, D_{90} = 35.38 ± 1.48 µm) as required for European intranasal formulations [30] (Fig. 1a and b). GCPQ preclinical toxicology studies produced an intranasal 28 day repeat dose no observed adverse effect level (NOAEL) of 18 mg kg^{-1}/day with minimal nasal cavity mucosal cell changes seen at 24 mg kg^{-1} [Supplementary Information (SI) SI Table 1]. The formulation is amorphous (SI Fig. 1a), stable for at least 90 days at room temperature (SI Fig. 1b–d) and delivers the peptide into the olfactory bulb and brain (Fig. 1c and d) on intranasal administration. Peptide brain delivery is mediated by the transport of the GCPQ nanoparticles into the olfactory neurons and further to the deeper brain regions of the thalamus and cortex (Fig. 2a–f, SI Fig. 2a and b), as imaged by Coherent Anti-Stokes Raman Scattering (CARS) microscopy [31] (with three animals sampled at all time points) and discussed below. Lochhead and others [32] have described the perivascular transport of fluorescent dextran to deep areas of the brain and their work provides evidence of a nose to brain transport pathway involving trigeminal neurons and perivascular arterial pathways. Our data supports the perivascular route of transport of these particles as perivascular located particles are indeed seen in the olfactory bulb (2b, yellow arrow) and cortex (2d, yellow arrow) CARS images, with red blood cells arrowed in white to locate the blood vessels. In our nanoparticle study, while particle entry to the olfactory neurons was shown in CARS images (Fig. 2a, yellow arrows – bottom of the image), we could not confirm particle transport via the respiratory epithelia/ trigeminal nerve pathway as is seen with the application of substances in solution [32,33].

There is no plasma exposure to the peptide when six animals were sampled at each time point (0.25, 0.5, 1 and 1.5 h) and this may be attributed to the very short peptide plasma half-life of 5–15 min [12]. Thus our data indicate that the intranasal particle approach allows exclusive delivery of this labile peptide to the brain. The nasal capillary pore size has been recently determined by Kumar and others [34] as:

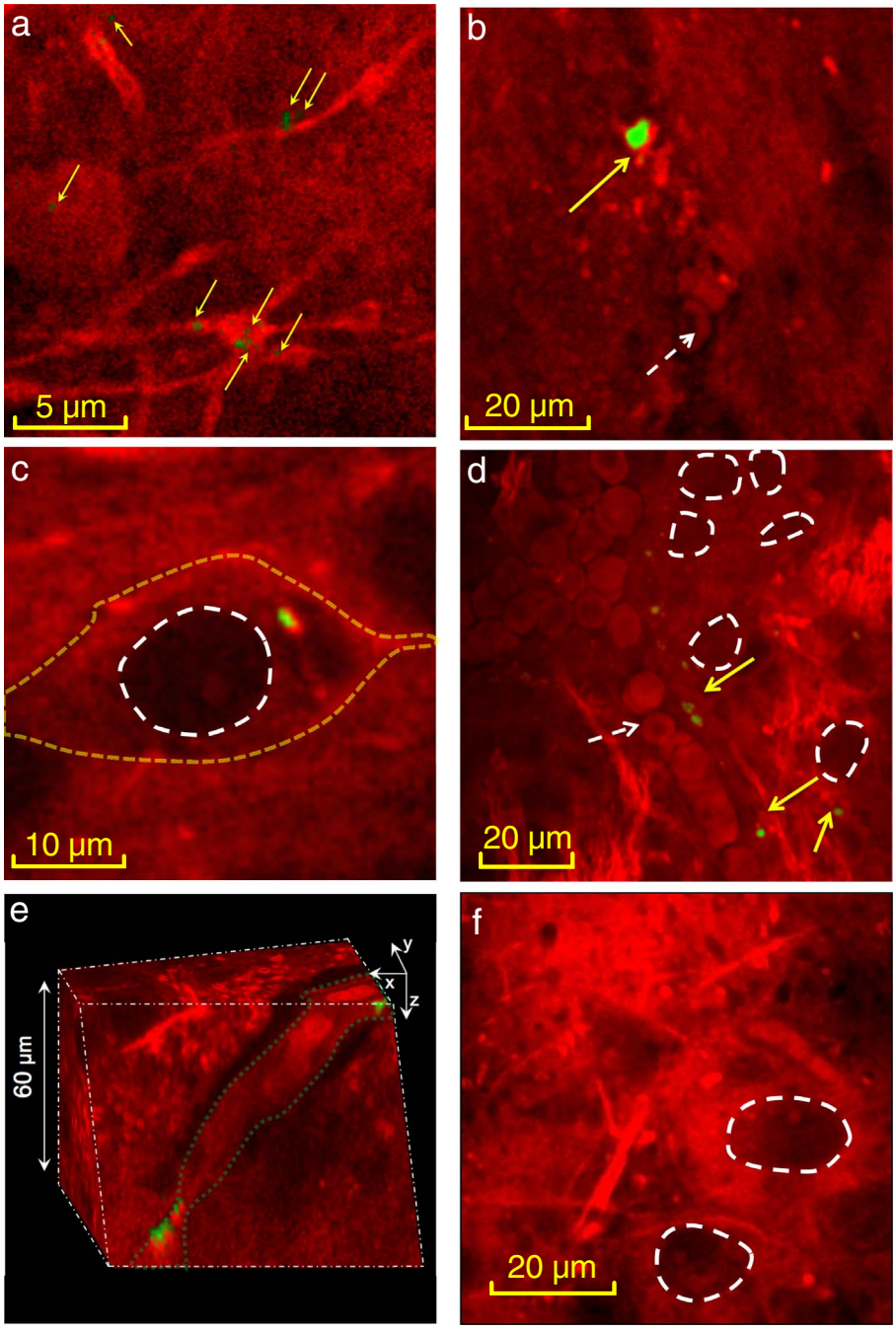

Fig. 2. Coherent Anti-Stokes Raman Spectroscopy (CARS) imaging of deuterated GCPQ (dGCPQ) nanoparticles in the brain following the intranasal administration in male SD rats (8.7 mg kg^{-1}, 40 mg mL^{-1}). Epi-detected dGCPQ CARS signal from the unique CD stretch (pump and Stokes tuned to excite 2100 cm^{-1}) is shown in green (also yellow arrows), while the non-specific counterstaining signal from the CH stretch (pump and Stokes tuned to excite 2845 cm^{-1}) appears in red. White dashed arrows highlight red blood cells within the blood vessels, while white dashed lines surround the edge of the nuclei. The dGCPQ signal is seen: a) in olfactory bulb neuritis in the nerve layer 5 min after dosing, b) in the olfactory bulb perivascular space 240 min after dosing, c) in the thalamus parenchyma 60 min after dosing (the cell membrane indicated by the dotted yellow line), d) the thalamus abluminal surface of the blood vessels and within the thalamus neurons 240 min after dosing, e) and in the perivascular space of the cortex 60 min after dosing (the edge of the blood vessel is delineated by a dashed green line and cross sections of neurons are seen at the top – y plane - of the image). f) No dGCPQ signal was seen in the basal ganglia 5 min after dosing. Data in Fig. 2 are representative images from 2 experiments, each comprising 3 animals at the relevant time points. (For interpretation of the references to colour in this figure legend, the reader is referred to the web version of this article.)

13–17 nm in the nasal respiratory vasculature and the olfactory bulb capillary pore size has been determined as < 10 nm in the olfactory bulb vasculature. This means that the transport of these 30–200 nm nanoparticles from the nasal cavity to the peripheral circulation and from the olfactory bulb to the peripheral circulation would be highly restricted, even though Nanomerics' MET nanoparticles are known to be taken up by epithelial cells [35]. However particles are seen on the abluminal surface of the thalamus blood vessels (Fig. 2d). The presence of particles in the abluminal surface of the thalamus blood vessels indicates that particle brain to blood transport in the thalamus is possible and we speculate that this is a probable route of particle/ polymer excretion.

Brain Cmax levels with nanoparticulate LENK were at 280 nM 30 min after dosing and are thus well in excess of the LENK kD values of 5 nM [36] and brain levels fell to 61 nM at the 90 min time point (Fig. 1d). However it must be stated that our analytical method did not allow us to distinguish between bound and free peptide. However unequivocal anti-nociceptive responses from multiple animal pain models does suggest that the peptide is available to bind to its receptors in the brain.

Kumar et al. reported anti-nociceptive data, with intranasal LENK trimethylchitosan formulations [37]. However no pharmacokinetics data were reported in this earlier study, and our data supplies crucial mechanistic detail in support of this earlier report.

Animal behavioural data demonstrate that NM0127 reverses hypersensitivity in the CFA model of inflammation-induced tactile hypersensitivity (Fig. 3a-f,) and produces relief of on going pain in a nerve injury model of neuropathic pain (Fig. 3g–h). The baseline paw withdrawal threshold in the CFA model, using von Frey filaments, ranged from 22.3 ± 5.7 to 26.0 ± 0 g, reducing to a range of 2.9 ± 1.2 to

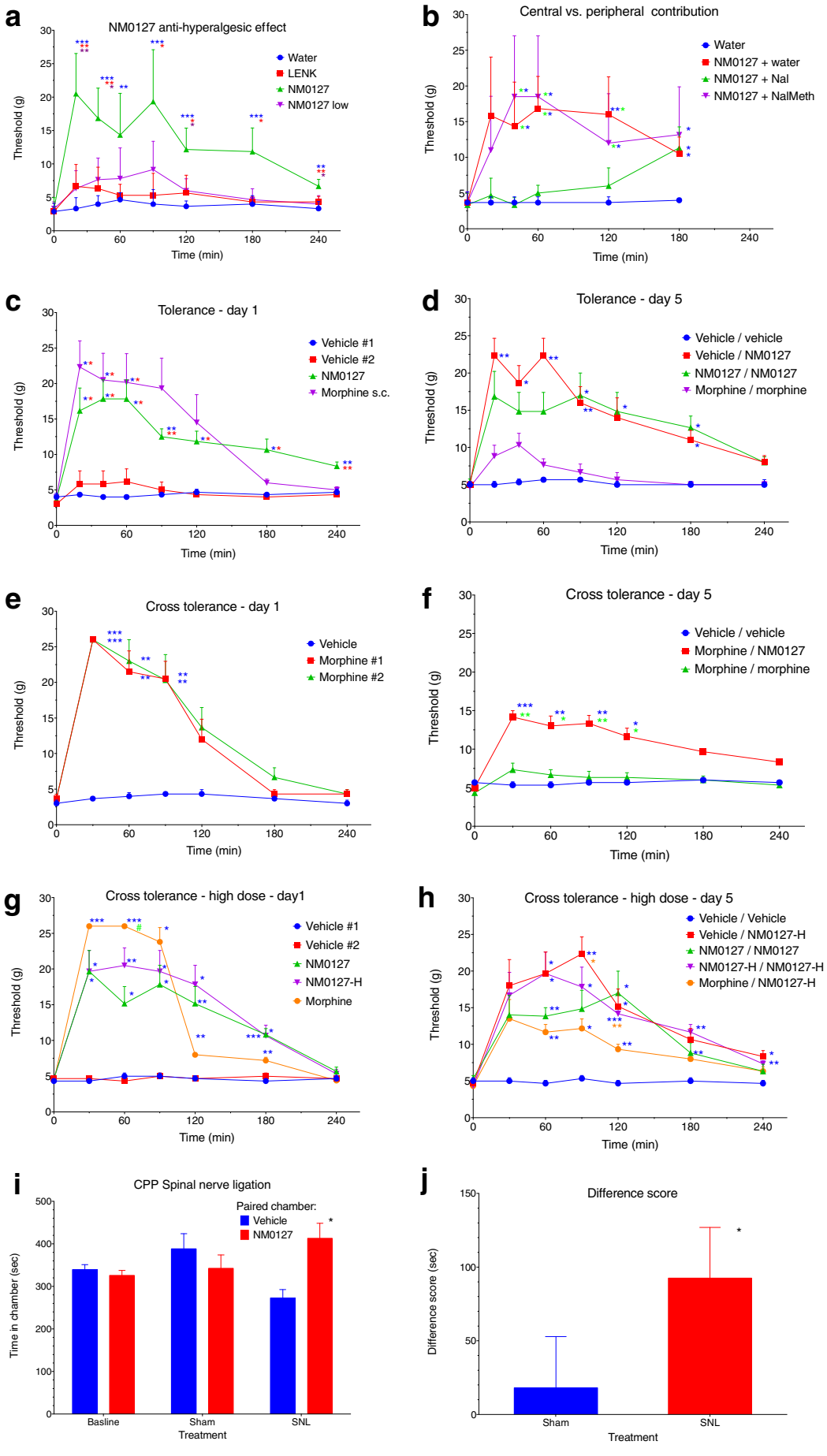

(caption on next page)

Fig. 3. Anti-hyperalgesic effects (mean ± sem) in male SD rats against evoked stimuli in a model of chronic inflammatory pain (CFA, a–f, n = 6) and against on going neuropathic pain in a conditioned placement preference model with spinal nerve ligation (SNL, i–j, n = 13–18). Evaluation parameters are kept constant throughout unless specified and LENK formulations were dosed at a pH of 5.8. Data in Fig. 3 is representative data from at least two replicated experiments. Statistically significant differences are given as: *** = $p < 0.001$, ** = $p < 0.01$, * = $p < 0.05$.

a) Hyperalgesia is assessed using response to pressure exerted with graded von Frey filaments before and 24 h after intraplantar injection of CFA (0.1 mL) in the hind paw. NM0127 = LENK given as GCPQ, LENK (ratio = 1 g g^{-1}, 7.5 mg kg^{-1}, 30 mg mL^{-1}), NM0127 Low = LENK given as GCPQ, LENK (ratio = 1 g g^{-1}, 3.5 mg kg^{-1}, 14 mg mL^{-1}), LENK = LENK solution (7.5 mg kg^{-1}), Water = water control (all volumes 0.25 mL kg^{-1}). Statistically significant differences between the NM0127 group and other groups were as follows: vs water (*** at 20, 40, 90, 120, 180 min; ** at 60, 240 min), vs LENK solution (** at 20, 40, 240 min; * at 90, 120, 180 min), vs NM0127 Low (** at 20 min, * at 40, 120, 240 min). The NM0127 Low group was not significantly different from the water group. Similar responses to the treatment and control formulations were recorded on Day 5 (data not shown).

b) Peripheral and central contributions to the anti-hyperalgesic effect of intranasal NM0127 were evaluated by comparing the intranasal water control group with intranasal NM0127 at a dose of 7.5 mg kg^{-1} combined with a concomitant subcutaneous injection (0.46 mL kg^{-1}) of either naloxone (Nal, 7.3 mg kg^{-1}), naloxone methiodide (NalMeth, 10 mg kg^{-1}), or water. Statistically significant differences were shown for: i) NM0127 + subcutaneous water and NM0127 + NalMeth vs both intranasal water and NM0127 + Nal (* at 30, 60, 120 min), ii) NM0127 + subcutaneous water vs intranasal water (** at 120 min), and iii) intranasal water vs all treatment groups (* at 180 min).

The development of analgesic tolerance was assessed by comparing the anti-hyperalgesic response to the first administration of the formulations on Day One (c) and on Day Five following 4 days of twice daily administration of the formulations (d).

c) On Day One statistically significant differences were shown between the subcutaneous morphine (7.5 mg kg^{-1}) vs the vehicle #1 (subcutaneous phosphate buffered saline, PBS, pH = 7.4) and vehicle #2 (intranasal PBS) groups (* at 15, 30, 60 min) and between the intranasal NM0127 (7.5 mg kg^{-1}) vs vehicle groups (** at 90, 240 min, * at 15, 30, 60, 120, 180 min).

d) On Day Five, animals (dosed on Day 1 and results shown in 3c) that had subsequently been administered formulations twice daily over 4 days – known as pre-treatment formulations were dosed with new formulations and their responses compared. Intranasal NM0127 was compared after pre-treatment with NM0127 (NM0127 + NM0127) or pre-treatment with intranasal vehicle (vehicle + NM0127) and these were both compared to subcutaneous morphine after morphine pre-treatment (morphine + morphine) and treatment with only the subcutaneous vehicle control group (vehicle + vehicle). Statistically significant differences were seen between the following pre-treatment + treatment combinations: vehicle + NM0127 vs vehicle + vehicle (** at 20, 60, 90 min; * at 40, 180 min), NM0127 + NM0127 vs vehicle + vehicle (* at 90, 120, 180 min), while morphine + morphine was not significantly different from vehicle + vehicle.

Cross-tolerance to morphine was also assessed by comparing anti-hyperalgesic responses pre- and post repeat administration as outlined above in Fig. 3c and d.

e) On Day One statistically significant differences were shown between the subcutaneous morphine #1 and morphine #2 groups (7.5 mg kg^{-1}) and the subcutaneous vehicle (PBS) group (*** at 30 min, ** at 60, 90 min).

f) On Day Five, animals (dosed on Day 1 and results shown in 3e) that had subsequently been administered formulations twice daily over 4 days – known as pre-treatment formulations were dosed with new formulations and their responses compared. Statistically significant differences were observed between the responses from the morphine (7.5 mg kg^{-1}) + NM0127 (7.5 mg kg^{-1}) and the subcutaneous vehicle + subcutaneous vehicle group (*** at 30 min, ** at 60, 90 min, * at 120 min) or the morphine + NM0127 and morphine + morphine groups (** at 30, 90 min, * at 60, 120 min). The morphine + morphine group was not significantly different from the vehicle control group.

Assessment of cross tolerance at higher doses was carried out as outlined above and responses on Day One (g) and Day Five (h) are shown.

g) On Day One, statistically significant differences were seen between: i) the vehicle #1 and vehicle #2 (both subcutaneous PBS) groups and the subcutaneous morphine (7.5 mg kg^{-1}) group (*** at 30, 60 min, ** at 120, 180 min, * at 90 min), ii) the vehicle groups and high dose NM0127 (NM0127-H, 15 mg kg^{-1} LENK, LENK concentration = 60 mg mL^{-1}, GCPQ, LENK ratio = 1: 1 g g^{-1}) group (** at 60 min, * 30, 90, 120, 180 min), iii) the vehicle groups and NM0127 (7.5 mg kg^{-1}) group (*** at 180 min, ** 120 min, * 30, 60, 90 min) and iv) the NM0127 and subcutaneous morphine groups ($^{\#} = p < 0.05$ at 60 min).

h) On Day Five, animals (dosed on Day 1 and results shown in 3 g) that had subsequently been administered formulations twice daily over 4 days – known as pre-treatment formulations were dosed with new formulations and their responses compared. Statistically significant differences were seen between: i) the subcutaneous vehicle control groups (vehicle + vehicle) and the vehicle + NM0127-H group (** at 90 min, * at 60, 120, 240 min), ii) the vehicle + vehicle group and the NM0127-H + NM0127-H group (*** at 120 min, ** at 180, 240 min, * at 60, 90 min), iii) the vehicle + vehicle group and the NM0127 + NM0127 (both at 7.5 mg kg^{-1}) groups (** at 60 min, * at 120 min), iv) the vehicle + vehicle and the morphine + NM0127-H group (** at 60, 120, 180 min, * at 90 min), v) the morphine + NM0127-H and the vehicle + NM0127-H groups (* at 90 min), and vi) the morphine + NM0127-H and the NM0127-H + NM0127-H groups (** at 120 min).

i) The effect of NM0127 against spontaneous pain in nerve injured rats (n = 13–18) was assessed in a conditioned placement preference model. The time spent in the drug paired chamber (red bars) and vehicle paired chamber (blue bars) did not differ at baseline, following sham treatment not involving spinal ligation ($p > 0.05$) and following spinal nerve ligation (SNL, $p > 0.05$). Therefore data were pooled for graphical representation. Following single trial conditioning with morning treatment with intranasal vehicle (0.25 mL kg^{-1}) and afternoon treatment 4 h later with intranasal NM0127 (GCPQ, LENK ratio = 1 g g^{-1}) at a LENK dose of 15 mg kg^{-1} (60 mg mL^{-1}) there was a statistically significant increase in the time spent in the NM0127 paired chamber selectively with SNL but not sham treated rats.

j) Comparison of the difference score (time in drug chamber at baseline – time in drug chamber following treatment) for both sham and SNL animals (n = 13–18) confirm that SNL treated rats show a significant increase in the time spent in the NM0127 paired chamber when compared to sham treated rats. * = Statistically significantly different when compared to sham treated rats ($p < 0.05$).

3.7 ± 1.5 g 24 h after the intraplantar injection of CFA (0.1 mL). 5 days after CFA dosing, the baseline paw withdrawal threshold ranged from 4.3 ± 0.3 to 5.7 ± 0.3 g. The baseline paw withdrawal thresholds, using von Frey filaments, for the sham and spinal ligation animals were 13.68 ± 0.72 g and 6.00 ± 0.82 g respectively.

Intranasal delivery of LENK encapsulated in GCPQ particles (NM0127) at a LENK dose of 7.5 mg kg^{-1} produced full reversal of CFA-induced tactile hypersensitivity. NM0127 reversal of CFA induced tactile hypersensitivity was only observed at LENK doses of 7.5 and 15 mg kg^{-1} (Fig. 3a–j) and not at a LENK dose of 3.5 mg kg^{-1} (Fig. 3a). Notably, intranasal administration of the LENK peptide alone is pharmacologically ineffective (Fig. 3a).

Although LENK is detected in the olfactory bulb when administered in solution (Fig. 1c), it is barely delivered to the brain when not encapsulated in nanoparticles (Fig. 1d), demonstrating that the nanoparticles facilitate the brain distribution to the thalamus and cortex, possibly via brain perivascular pathways [32] (Fig. 2b and e). The nanoparticles are thus instrumental in delivering the peptide to the brain. The polymer used to make the nanoparticles normally confers a positive surface charge to the nanoparticles and the particles are known to stick to and integrate into mucosal surfaces [38], which are likely to be present in the nasal cavity and we speculate that the mucointegration may enhance the residence time of the nanoparticulate peptide in the nares. This mucointegration would contribute to the pharmacodynamics effects observed. Intravenous LENK alone is also incapable of mediating an anti-nociceptive response (SI Fig. S1e) with only intravenous NM0127 being active. These observations indicate pharmacological activity is only obtained with the nanoparticle formulation and is not obtained with the peptide alone. The NM0127 reversal of CFA – induced tactile hypersensitivity is blocked by the opiate receptor antagonist naloxone but not by the peripherally restricted [39] quaternary ammonium inhibitor - naloxone methiodide (Fig. 3b). When this data is viewed in combination with the lack of peripheral exposure to LENK, we conclude that intranasal GCPQ nanoparticles may be used to deliver LENK exclusively to the brain. By the 3 h time point naloxone was no longer active (Fig. 3b) due presumably to its short plasma half-life of 30–40 min in rats [40] and the anti-nociceptive activity of NM0127 is restored.

While demonstrating the delivery potential of the nanoparticle formulation is important, NM0127 also exhibits some potentially

significant advantages over the current MOR agonists. Approximately 40–95% of MOR agonist patients develop constipation [11], which is largely peripherally mediated [41] and as such peripherally restricted MOR antagonists have been developed to control the constipation side effect [42]. The centrally restricted activity of NM0127 has a good probability of addressing this major side effect.

Analgesic tolerance is a major side effect of MOR agonist use: 1 in 12 admissions in a Boston hospital study were patients tolerant to opioids and opioid tolerance was associated with a longer hospital stay in these patients [43]. Opioid tolerance is known to be very difficult to manage [44]. Our data demonstrate that analgesic tolerance does not develop to NM0127 (Fig. 3c and d) and that NM0127 is active in morphine tolerant animals (Fig. 3e–h). Additionally chronic morphine dosing produced immediate hyperactivity post dosing, with hyperactivity beginning 2 min after dosing on Day 4, and such hyperactivity was not observed in the NM0127 dosed animals (data not shown). The molecular mechanisms of opioid analgesic tolerance are poorly understood [45,46] and future studies will seek to understand the lack of analgesic tolerance shown by NM0127.

Finally we show for the first time that intranasal LENK nanoparticles induce conditioned placement preference selectively in animals, with spinal nerve ligation injury, suggesting blockade of on going neuropathic pain (Fig. 3i and j). It should be noted that animals with sham surgery do not show place conditioning to NM0127, suggesting no to minimal reward seeking behaviour after a single intranasal dose of NM0127. Further experiments with validated addiction models are required for this lack of reward seeking behaviour to be confirmed.

4. Conclusions

In summary, we introduce nanotechnology, with accompanying short term stability data, which has the potential to be scaled up into a pharmaceutical product, using industrially relevant equipment and processes (high pressure homogenisation and spray drying). The nanotechnology enables the exclusive delivery of a metabolically labile peptide drug into the brain on intranasal delivery. Unexpected pharmacological evidence of activity of the delta selective opioid agonist (LENK) in morphine tolerant animals was also uncovered. We also provide evidence that these nanoparticles may be presented as a microparticle based powder to satisfy regulatory requirements and that the nanoparticle polymer is well tolerated via the nasal route at the dose administered.

Acknowledgements

Charles River, Edinburgh, UK is acknowledged for the conduct of the conduct of the GCPQ nanoparticles GLP repeat dose toxicology studies.

The UK Engineering and Physical Sciences Research Council(EP/K502340/1), Nanomerics Ltd.(NM12TSB-NPP) and Innovate UK (16939-124181) are acknowledged for funding.

Author contributions

Ijeoma F. Uchegbu, Andreas G. Schätzlein, Lisa Godfrey, Tamara King, Frank Porreca, Antonio Iannitelli, Julian Moger and Natalie Garrett conceived and designed the experiments. Ijeoma Uchegbu and Lisa Godfrey wrote the manuscript and analysed the data. Lisa Godfrey, Tamara King, Antonio Iannitelli, Natalie Garrett, Aikaterini Lalatsa, Ian Imbert and Ramesh Soundararajan performed the experiments and analysed the data. All authors reviewed the manuscript prior to publication.

Appendix A. Supplementary data

Supporting information contains stability data on NM0127 and data from the safety studies on the self-assembling nanoparticle forming polymer. Supplementary data associated with this article can be found in the online version, at https://doi.org/10.1016/j.jconrel.2017.11.041.

References

[1] M. Mazza, R. Notman, J. Anwar, A. Rodger, M. Hicks, G. Parkinson, D. McCarthy, T. Daviter, J. Moger, N. Garrett, T. Mead, M. Briggs, A.G. Schatzlein, I.F. Uchegbu, Nanofiber-based delivery of therapeutic peptides to the brain, ACS Nano 7 (2013) 1016–1026.
[2] C.D. Chapman, W.H. Frey II, S. Craft, L. Danielyan, M. Hallschmid, H.B. Schioth, C. Benedict, Intranasal treatment of central nervous system dysfunction in humans, Pharm. Res. 30 (2013) 2475–2484.
[3] M.A. Hussain, S.M. Rowe, A.B. Shenvi, B.J. Aungst, Inhibition of leucine enkephalin metabolism in rat blood, plasma and tissues in vitro by an aminoboronic acid derivative, Drug Metab. Dispos. 18 (1990) 288–291.
[4] H.W. Kosterlitz, Enkephalins, endorphins and their receptors, in: C.A. Marsen, W.Z. Traczyk (Eds.), Neuropeptides and Neural Transmission, Raven Press, New York, 1980.
[5] L. Toll, I.P. Berzetei-Gurske, W.E. Polgar, S.R. Brandt, I.D. Adapa, L. Rodriguez, R.W. Schwartz, D. Haggart, A. O'Brien, A. White, J.M. Kennedy, K. Craymer, L. Farrington, J.S. Auh, Standard binding and functional assays related to medications development division testing for potential cocaine and opiate narcotic treatment medications, NIDA Res. Monogr. 178 (1998) 440–466.
[6] J. Peng, S. Sarkar, S.L. Chang, Opioid receptor expression in human brain and peripheral tissues using absolute quantitative real-time RT-PCR, Drug Alcohol Depend. 124 (2012) 223–228.
[7] H. Breivik, B. Collett, V. Ventafridda, R. Cohen, D. Gallacher, Survey of chronic pain in Europe: prevalence, impact on daily life, and treatment, Eur. J. Pain 10 (2006) 287–333.
[8] S. Nightingale, The neuropathic pain market, Nat. Rev. Drug Discov. 11 (2012) 102–103.
[9] R.K. Portenoy, D.S. Bennett, R. Rauck, S. Simon, D. Taylor, M. Brennan, S. Shoemaker, Prevalence and characteristics of breakthrough pain in opioid-treated patients with chronic noncancer pain, J. Pain 7 (2006) 583–591.
[10] G.W. Pasternak, Y.X. Pan, Mu opioids and their receptors: evolution of a concept, Pharmacol. Rev. 65 (2013) 1257–1317.
[11] R. Benyamin, A.M. Trescot, S. Datta, R. Buenaventura, R. Adlaka, N. Sehgal, S.E. Glaser, R. Vallejo, Opioid complications and side effects, Pain Physician 11 (2008) S105–120.
[12] G. Roscetti, R. Possenti, E. Bassano, L.G. Roda, Mechanisms of leu-enkephalin hydrolysis in human plasma, Neurochem. Res. 10 (1985) 1393–1404.
[13] L. Churchill, H.H. Bausback, M.E. Gerritsen, P.E. Ward, Metabolism of opioid peptides by cerebral microvascular aminopeptidase M, Biochim. Biophys. Acta 923 (1987) 35–41.
[14] A. Lalatsa, A.G. Schatzlein, I.F. Uchegbu, Strategies to deliver peptide drugs to the brain, Mol. Pharm. 11 (2014) 1081–1093.
[15] A. Lalatsa, N. Garrett, J. Moger, A.G. Schatzlein, C. Davis, I.F. Uchegbu, Delivery of peptides to the blood and brain after oral uptake of quaternary ammonium palmitoyl glycol chitosan nanoparticles, Mol. Pharm. 9 (2012) 1764–1774.
[16] A. Lalatsa, V. Lee, J.P. Malkinson, M. Zloh, A.G. Schatzlein, I.F. Uchegbu, A prodrug nanoparticle approach for the oral delivery of a hydrophilic peptide, leucine(5)-enkephalin, to the brain, Mol. Pharm. 9 (2012) 1665–1680.
[17] B.P. Roques, M.C. Fournie-Zaluski, M. Wurm, Inhibiting the breakdown of endogenous opioids and cannabinoids to alleviate pain, Nat. Rev. Drug Discov. 11 (2012) 292–310.
[18] L. Illum, Is nose-to-brain transport of drugs in man a reality? J. Pharm. Pharmacol. 56 (2004) 3–17.
[19] K. Ohkubo, J.N. Baraniuk, M. Merida, J.N. Hausfeld, H. Okada, M.A. Kaliner, Human nasal mucosal carboxypeptidase: activity, location, and release, J. Allergy Clin. Immunol. 96 (1995) 924–931.
[20] X. Zhang, Q.Y. Zhang, D. Liu, T. Su, Y. Weng, G. Ling, Y. Chen, J. Gu, B. Schilling, X. Ding, Expression of cytochrome p450 and other biotransformation genes in fetal and adult human nasal mucosa, Drug Metab. Dispos. 33 (2005) 1423–1428.
[21] A. Fortuna, G. Alves, A. Serralheiro, J. Sousa, A. Falcao, Intranasal delivery of systemic-acting drugs: small-molecules and biomacromolecules, Eur. J. Pharm. Biopharm. 88 (2014) 8–27.
[22] S.T. Charlton, S.S. Davis, L. Illum, Nasal administration of an angiotensin antagonist in the rat model: effect of bioadhesive formulations on the distribution of drugs to the systemic and central nervous systems, Int. J. Pharm. 338 (2007) 94–103.
[23] S. Orita, T. Ishikawa, M. Miyagi, N. Ochiai, G. Inoue, Y. Eguchi, H. Kamoda, G. Arai, T. Toyone, Y. Aoki, T. Kubo, K. Takahashi, S. Ohtori, Pain-related sensory innervation in monoiodoacetate-induced osteoarthritis in rat knees that gradually develops neuronal injury in addition to inflammatory pain, BMC Musculoskelet. Disord. 12 (2011) 134.
[24] W.J. Dixon, Efficient analysis of experimental observations, Ann. Rev. Pharmacol. Toxicol. 20 (1980) 441–462.
[25] S.H. Kim, J.M. Chung, An experimental model for peripheral neuropathy produced by segmental spinal nerve ligation in the rat, Pain 50 (1992) 355–363.
[26] T. King, L. Vera-Portocarrero, T. Gutierrez, T.W. Vanderah, G. Dussor, J. Lai, H.L. Fields, F. Porreca, Unmasking the tonic-aversive state in neuropathic pain, Nat. Neurosci. 12 (2009) 1364–1366.
[27] R. Wang, T. King, M. De Felice, W. Guo, M.H. Ossipov, F. Porreca, Descending

facilitation maintains long-term spontaneous neuropathic pain, J. pain 14 (2013) 845–853.
[28] N.L. Garrett, A. Lalatsa, I. Uchegbu, A. Schatzlein, J. Moger, Exploring uptake mechanisms of oral nanomedicines using multimodal nonlinear optical microscopy, J. Biophotonics 5 (2012) 458–468.
[29] J.D. Belluzzi, N. Grant, V. Garsky, D. Sarantakis, C.D. Wise, L. Stein, Analgesia induced in vivo by central administration of enkephalin in rat, Nature 260 (1976) 625–626.
[30] European Medicines Agency, Committee for Medicinal Products for Human Use - Guideline on the Pharmaceutical Quality of Inhalation and Nasal Products, http://www.ema.europa.eu/docs/en_GB/document_library/Scientific_guideline/2009/09/WC500003568.pdf, (2006).
[31] J. Moger, N.L. Garrett, D. Begley, L. Mihoreanu, A. Lalatsa, M. Lozano, M. Mazza, A. Schatzlein, I.F. Uchegbu, Imaging cortical vasculature with stimulated Raman scattering and two photon photothermal lensing microscopy, J. Raman Spectrosc. 43 (2012) 668–674.
[32] J.J. Lochhead, D.J. Wolak, M.E. Pizzo, R.G. Thorne, Rapid transport within cerebral perivascular spaces underlies widespread tracer distribution in the brain after intranasal administration, J. Cereb. Blood Flow Metab. 35 (2015) 371–381.
[33] N.J. Johnson, L.R. Hanson, W.H. Frey, Trigeminal pathways deliver a low molecular weight drug from the nose to the brain and orofacial structures, Mol. Pharm. 7 (2010) 884–893.
[34] N.N. Kumar, M. Gautam, J.J. Lochhead, D.J. Wolak, V. Ithapu, V. Singh, R.G. Thorne, Relative vascular permeability and vascularity across different regions of the rat nasal mucosa: implications for nasal physiology and drug delivery, Sci. Rep. 6 (2016) 31732.
[35] D.R. Serrano, A. Lalatsa, M.A. Dea-Ayuela, P.E. Bilbao-Ramos, N.L. Garrett, J. Moger, J. Guarro, J. Capilla, M.P. Ballesteros, A.G. Schatzlein, F. Bolas, J.J. Torrado, I.F. Uchegbu, Oral particle uptake and organ targeting drives the activity of amphotericin B nanoparticles, Mol. Pharm. 12 (2015) 420–431.
[36] A.J. Blume, J. Shorr, J.P. Finberg, S. Spector, Binding of the endogenous nonpeptide morphine-like compound to opiate receptors, Proc. Natl. Acad. Sci. U. S. A. 74 (1977) 4927–4931.
[37] M. Kumar, R.S. Pandey, K.C. Patra, S.K. Jain, M.L. Soni, J.S. Dangi, J. Madan, Evaluation of neuropeptide loaded trimethyl chitosan nanoparticles for nose to brain delivery, Int. J. Biol. Macromol. 61 (2013) 189–195.
[38] A. Siew, H. Le, M. Thiovolet, P. Gellert, A. Schatzlein, I. Uchegbu, Enhanced oral absorption of hydrophobic and hydrophilic drugs using quaternary ammonium palmitoyl glycol chitosan nanoparticles, Mol. Pharm. 9 (2012) 14–28.
[39] W.T. Chance, J.L. Nelson, Antagonism of stress-induced analgesia by quaternary naloxone, Brain Res. 380 (1986) 394–396.
[40] S.H. Ngai, B.A. Berkowitz, J.C. Yang, J. Hempstead, S. Spector, Pharmacokinetics of naloxone in rats and in man: basis for its potency and short duration of action, Anesthesiology 44 (1976) 398–401.
[41] T. Mori, Y. Shibasaki, K. Matsumoto, M. Shibasaki, M. Hasegawa, E. Wang, D. Masukawa, K. Yoshizawa, S. Horie, T. Suzuki, Mechanisms that underlie mu-opioid receptor agonist-induced constipation: differential involvement of mu-opioid receptor sites and responsible regions, J. Pharmacol. Exp. Ther. 347 (2013) 91–99.
[42] J.A. Cassel, J.D. Daubert, R.N. DeHaven, H-3 alvimopan binding to the mu opioid receptor: comparative binding kinetics of opioid antagonists, Eur. J. Pharmacol. 520 (2005) 29–36.
[43] P. Gulur, L. Williams, S. Chaudhary, K. Koury, M. Jaff, Opioid tolerance—a predictor of increased length of stay and higher readmission rates, Pain Physician 17 (2014) E503–507.
[44] J.L. Wilson, P.A. Poulin, R. Sikorski, H.J. Nathan, M. Taljaard, C. Smyth, Opioid use among same-day surgery patients: prevalence, management and outcomes, Pain Res. Manag. 20 (2015) 300–304.
[45] R. Al-Hasani, M.R. Bruchas, Molecular mechanisms of opioid receptor-dependent signaling and behavior, Anesthesiology 115 (2011) 1363–1381.
[46] A.A. Pradhan, W. Walwyn, C. Nozaki, D. Filliol, E. Erbs, A. Matifas, C. Evans, B.L. Kieffer, Ligand-directed trafficking of the delta-opioid receptor in vivo: two paths toward analgesic tolerance, J. Neurosci. 30 (2010) 16459–16468.